In Vivo Calpain/Caspase Cross-talk during 3-Nitropropionic Acid-induced Striatal Degeneration

Nicolas Bizat, Jean-Michel Hermel, Sandrine Humbert, Carine Jacquard,
Christophe Créminon, Carole Escartin, Frédéric Saudou, Stan Krajewski,
Philippe Hantraye, Emmanuel Brouillet

In Vivo Calpain/Caspase Cross-talk during 3-Nitropropionic Acid-induced Striatal Degeneration

IMPLICATION OF A CALPAIN-MEDIATED CLEAVAGE OF ACTIVE CASPASE-3*

Nicolas Bizat‡, Jean-Michel Hermel‡§, Sandrine Humbert§¶, Carine Jacquard‡,
Christophe Créminon**, Carole Escartin‡, Frédéric Saudou¶‖‡‡, Stan Krajewski§§,
Philippe Hantraye‡¶¶, and Emmanuel Brouillet‡‖‖‖

*From the ‡Unité de Recherche Associée Commissariat à l'Energie Atomique (CEA)-CNRS 2210, Service Hospitalier Frédéric Joliot, Département de Recherches Médicales (DRM), Direction des Sciences du Vivant (DSV), Commissariat à l'Energie Atomique, 91401 Orsay Cedex, France, ¶UMR 146 CNRS/Institut Curie, 91405 Orsay, France, **CEA, Service de Pharmacologie et Immunologie, DRM, DSV, CEN Saclay, 91191 Gif-sur-Yvette Cedex, France, §§Program on Cell Death and Apoptosis, The Burnham Institute, Program on Apoptosis, Cell Death and Aging, La Jolla, California 92037, and ¶¶Isotopic Imaging, Biochemical and Biophysical Unit (U2IBP), Service Hospitalier Frédéric Joliot, DRM, DSV, CEA, 91401 Orsay Cedex, France*

The role of caspases and calpains in neurodegeneration remains unclear. In this study, we focused on these proteases in a rat model of Huntington's disease using the mitochondrial toxin 3-nitropropionic acid (3NP). Results showed that 3NP-induced death of striatal neurons was preceded by cytochrome *c* redistribution, transient caspase-9 processing, and activation of calpain, whereas levels of the active/processed form of caspase-3 remained low and were even reduced as compared with control animals. We evidenced here that this decrease in active caspase-3 levels could be attributed to calpain activation. Several observations supported this conclusion. 1) Pharmacological blockade of calpain in 3NP-treated rats increased the levels of endogenous processed caspase-9 and caspase-3. 2) Cell-free extracts prepared from the striatum of 3NP-treated rats degraded *in vitro* the p34 and p20 subunits of active recombinant caspase-9 and caspase-3, respectively. 3) This degradation of p34 and p20 could be mimicked by purified μ-calpain and was prevented by calpain inhibitors. 4) μ-Calpain produced a loss of the DEVDase (Asp-Glu-Val-Asp) activity of active caspase-3. 5) Western blot analysis and experiments with ^{35}S-radiolabeled caspase-3 showed that μ-calpain cleaved the p20 subunit of active caspase-3 near its catalytic site. 6) μ-Calpain activity was selectively inhibited (IC_{50} of 100 μM) by a 12 amino acid peptide corresponding to the C terminus of p20. Our results showed that calpain can down-regulate the caspase-9/caspase-3 cell death pathway during neurodegeneration due to chronic mitochondrial defects *in vivo* and that this effect may involve, at least in part, direct cleavage of the caspase-3 p20 subunit.

Several evidences demonstrate the role of excitotoxic cell death and mitochondrial defects in neurodegenerative diseases (1). This hypothesis is strongly supported for Huntington's disease (HD),[1] an inherited neurodegenerative disorder caused by an abnormal expansion of a polyglutamine tract in the huntingtin (Htt) protein (2). HD is characterized by involuntary choreiform movements and cognitive deficits (3). The most striking neuropathological characteristic of this disorder is preferential atrophy of the striatum due to death of medium size spiny neurons (3).

The involvement of excitotoxicity in HD was initially supported by observations that several histological and behavioral anomalies of HD can be mimicked in rats and non-human primates by intrastriatal injection of agonists of the glutamate receptors (4), in particular quinolinate, an agonist of the *N*-methyl-D-aspartate (NMDA) subtype of glutamate receptors (5, 6). Anomalies in the NMDA-evoked current amplitude have been observed in transgenic mice for the mutated full-length Htt, further substantiating the "excitotoxic" hypothesis (7, 8). In addition, the striatum in these HD transgenic mice exhibits increased vulnerability to the toxicity of quinolinate (8).

It has been suggested that excitotoxic neuronal death could be an indirect consequence of the chronic mitochondrial anomalies that have consistently been reported in HD patients (9, 10). Thus, decreases in the activity of respiratory chain complex II (11, 12) and increases in lactate concentrations have been evidenced in the striatum of HD patients (13). Mitochondria from lymphoblasts of HD patient also display increased vulnerability to apoptotic stimuli (14), anomalies in mitochondrial membrane potential, and defect in Ca^{2+}-buffering capacity (15).

Observations using the mitochondrial toxin 3-nitropropionic acid (3NP), an irreversible inhibitor of succinate dehydrogenase/complex II (16), also support the so-called "indirect excitotoxic" hypothesis for HD. Indeed, chronic systemic administration of 3NP in rats and non-human primates produces homogenous blockade of complex II within the brain (17), leading to preferential excitotoxic striatal degeneration associated

---

§ Both authors contributed equally to this work.
‖ Investigators from INSERM.
‡‡ An EMBO Young Investigator.
‖‖‖ To whom correspondence should be addressed. Tel.: 33-1-69-86-78-15; Fax: 33-1-69-86-77-45; E-mail: brouille@shfj.cea.fr.

[1] The abbreviations used are: HD, Huntington's Disease; Htt, huntingtin; ANOVA, analysis of variance; CHO, C-terminal aldehyde form; CI-1, calpain inhibitor I; NMDA, *N*-methyl-D-aspartate; Ct12p20, C terminus of caspase-3 p20; SDH, succinate dehydrogenase; 3NP, 3-nitropropionic acid; cyt *c*, cytochrome *c*; AMC, 7-amino-4-methyl-coumarin; AFC, 7-amino-4-trifluoro-methyl-coumarin; DEVD, Asp-Glu-Val-Asp; LEHD, Leu-Glu-His-Asp.

Calpain/Caspase-3 Cross-talk during Neurodegeneration

with behavioral abnormalities that are highly reminiscent of HD (18–20).

Despite numerous published studies, the cell death mechanisms underlying 3NP neurotoxicity *in vivo* are not fully understood (21). We recently examined the involvement of death proteases of the caspase family and Ca^{2+}-activated neutral protease calpains in 3NP toxicity in rats (22). Interestingly, we found that when 3NP was administered to produce a chronic/steady mitochondrial perturbation, caspase-9 was transiently activated but surprisingly without being followed by an increased activation of caspase-3. In contrast, abnormal activation of the Ca^{2+}-activated neutral protease calpain was observed in the striatum of 3NP-treated rats (22), as seen in the striatum of HD patients (23). The reasons that could account for the predominance of calpain over caspase-3 despite a transient activation of caspase-9 in the 3NP model of degeneration remained speculative assumptions (22).

In this study, we further examined the mechanisms involved in the predominance of calpain over caspase-3 activation in the chronic 3NP model of HD. Because elegant experiments recently demonstrated the existence of a complex cross-talk between calpains and caspases (24–27), we hypothesized that calpain could play an important role in the stoppage of the mitochondrial caspase pathway in this chronic 3NP lesion model. Using this model, we re-examined the time course of activation of calpain and caspase-9 and caspase-3 and we studied how calpain could modify the caspase-9/caspase-3 pathway *in vivo* and *in vitro*. We provide hereforth the biochemical and pharmacological evidences that in this model calpain inactivates the caspase-9/caspase-3 pathway through, at least partly, direct proteolysis of their active forms. In particular, calpain inactivates active caspase-3 by cleaving the C terminus domain of its p20 subunit.

MATERIALS AND METHODS

Animals—Because 3NP toxicity is age-dependent (28), all of the experiments were carried out in 12-week-old male Lewis rats (IFFA Credo, L'Arbresle, France) weighing 340–370 g. Experimental procedures were performed in strict compliance with the recommendations of the European Community (86/609/EEC) and the French National Committee (87/848) for care and use of laboratory animals.

Chemical and Reagents—All of the chemicals and reagents were purchased from Sigma unless specified.

3NP Treatment and Experimental Design—As described previously, a solution of 3NP was systemically delivered by chronic infusion (54 mg/kg/day) using osmotic mini-pumps (flow rate 10 μl/h, model 2ML1, Alzet Inc, Palo Alto, CA) placed subcutaneously in the back of the rats under ketamine-xylazine anesthesia (22, 29, 30). Control rats were sham-operated. Groups of rats ($n = 5$–8) were killed by decapitation at daily intervals (days 1, 2, 3, 4, and 5) after osmotic pump implantation (day 0). In one experiment, animals ($n = 5$/time point) were killed every 6 h from day 2 to 5.

Motor Score—Animals were observed daily to detect the occurrence of motor symptoms. Each animal was scored using a neurological scale (normal = 0, very symptomatic = 8) as previously described (29, 30).

Calpain Inhibitor I Neuroprotection Experiments in the Chronic Model—The calpain inhibitor I (CI-1, z-Leu-Leu-Norleucinal, Biomol, Plymouth Meeting, PA) solubilized in dimethyl sulfoxide (40%) and diluted in phosphate-buffered saline were delivered (infusion rate 2.5 μg·μl^{-1}·h^{-1}) by intra-cerebroventricular infusion using an osmotic mini-pump (Model 2001, Alzet) connected to a stereotaxically implanted cannula (antero-posterior = -1.6 mm; lateral = 2.0 mm from Bregma; ventral = 3.5 mm from Dura; "brain infusion kit," Alzet) (22). The osmotic pump delivering CI-1 and that delivering 3NP were implanted simultaneously. Biochemical analyses were performed on day 5 of the neurotoxic treatment.

Brain Processing, Sample Dissection, and Homogenization—Brains were rapidly removed from the skull and cut vertically along the rostrocaudal axis into two hemispheres. The left hemisphere was fixed in Bouin's solution for 3 days and paraffin-embedded for immunohistochemical evaluation. Striatum samples were dissected from the right hemisphere and processed for biochemical analyses. Tissue dissection

and processing were performed at 4 °C. The lateral striatum was dissected out of a 2-mm-thick coronal slice. Tissue samples (10–20 mg) were homogenized using a 1-ml glass Teflon potter (900 rpm, 20 strokes) in 300 μl of buffer containing protease inhibitor mixture (Complete, Roche Applied Science). For cytochrome c (cyt c) redistribution studies, homogenization was performed in buffer A preserving mitochondria (10 mM HEPES-KOH, pH 7.4, 60 mM sucrose, 210 mM mannitol, 5 mM EGTA, 1 mM EDTA, 10 mM KCl, 10 mM succinate, and 1 mM ADP). For evaluation of caspase-3 and caspase-9 and calpain activities during the course of the 3NP treatment, homogenization was performed in buffer B containing 250 mM sucrose, 1 mM EDTA, 50 mM Tris-HCl, pH 7.4, and 1 mM dithiothreitol as previously described (31). Homogenate was first centrifuged at 1000 $\times$ g for 5 min. The post-nuclear supernatant was centrifuged at 15,000 $\times$ g for 30 min, the resulting pellet containing the mitochondria fraction. The supernatant was further centrifuged at 100,000 $\times$ g for 30 min. The resulting high speed supernatant contained the cytosol fraction, whereas the high speed pellet contained the membrane fraction. In cell-free extract studies examining calpain/caspase cross-talk, fractions enriched in cytosol were prepared by homogenization in a buffer C containing 25 mM HEPES-KOH, pH 7.4, 0.1% Triton X-100, 5 mM MgCl$_2$, 1.3 mM EDTA, and 1 mM EGTA (22). This homogenate was centrifuged at 15,000 $\times$ g for 30 min, giving a cell-free extract (supernatant) and a membrane-enriched fraction (pellet). This procedure led to essentially similar results in terms of protease activities when compared with the use of buffer B with a three-step centrifugation. All of the fractions were stored at -80 °C until analysis.

Histological Studies—Hoechst nuclear staining with bis-benzimide H33258 and histochemistry for cyt c (primary antibody against cyt c, BD Biosciences) were performed on paraffin sections as described previously (22, 32). Histochemistry of succinate dehydrogenase (SDH) was performed and quantitatively analyzed according to previously published procedures (17, 22, 29).

Western Blot Analysis—Protein concentrations were determined using the BCA method (Pierce) according to the manufacturer's instructions. Proteins in striatal samples were separated by SDS-PAGE as described previously (22). Following blot transfer, nitrocellulose membranes were incubated overnight at 4 °C with one of the antibodies raised against the following: fodrin (1:2000, antibody against non-erythroid α-spectrin, Chemicon, Temecula, CA), cytochrome c (1:2000; BD Biosciences, San Diego, CA), calbindin D28k (1:1000, monoclonal, Sigma), caspase-9 (1:1000, rabbit polyclonal Bur 81, Burnham Institute) (32), and C-terminal domain of active caspase-3 p20 subunit (1:1000, rabbit polyclonal antibody 1797, Cell Signaling Technology, Beverly, MA). After incubation with the primary antibody, the blots were incubated with horseradish peroxidase-conjugated anti-mouse or anti-rabbit IgG (1:1000, Sigma) and peroxidase activity was detected using ECL reagent (Amersham Biosciences). For detection of active caspase-3 in cytosolic fractions of the striatum of 3NP-treated rats prepared by ultracentrifugation (see time-course study in Fig. 3), secondary antibody was used at 1:5000 dilution and peroxidase activity was detected using Femto-ECL reagent (Pierce).

Oligonucleosome Detection—Oligonucleosome contents in soluble fractions (20 μl) were determined using the enzyme-linked immunosorbent assay cell death detection kit (Roche Applied Science) according to the manufacturer's instructions. The results were normalized by the protein concentration in each sample and expressed as mean the optical density values $\pm$ S.E.

Proteolytic Activity Assay Using Fluorogenic Substrate for Caspase and Calpain—The fluorescent assay of proteases is based on the cleavage of 7-amino-4-methyl-coumarin (AMC) or 7-amino-4-trifluoro-methyl-coumarin (AFC) dyes from the C terminus of the peptide substrates (22). The calpain activity was determined using *N*-succinyl-Leu-Tyr-(*N*-succinyl-LY)-AMC, a substrate preferentially cleaved by μ-calpain and m-calpain (33). Calpain activity (Ca^{2+}-dependent cleavage of *N*-succinyl-LY-AMC) present in cytosol fraction (10 μl containing ~30 μg of protein) was determined as the difference between the calcium-dependent and the non-calcium-dependent fluorescence. The calcium-dependent fluorescence released was measured after a 30-min incubation at 37 °C in buffer D containing 63 mM imidazole-HCl, pH 7.3, 10 mM β-mercaptoethanol, and 5 mM CaCl$_2$ and is attributable to the cleavage of 150 μM *N*-succinyl-LY-AMC. The non-calcium-dependent fluorescence was measured under the same conditions using buffer D without calcium and containing 1 mM EDTA and 10 mM EGTA. Using the fluorometric assay described above, we performed *in vitro* concentration-dependent inhibition experiments of calpain activity (purified μ-calpain, 0.2 units/well, Calbiochem) with the synthetic peptide corresponding to the 12 amino acids of the C terminus of caspase-3 p20 (Ct12p20,

RGTELDCGIETD), a scramble peptide (ICDLGTEDRTEG), and a peptide with leucine 168 substituted by a lysine (Ct12p20-L168K, RGTEK-DCGIETD) solubilized at 10 mM (90% pure) in water.

Caspases-3, -8, and -9 activities were tested on peptidic substrates (Biomol) using, respectively, *N*-acetyl-Asp-Glu-Val-Asp-AFC (DEVD-AFC), *N*-acetyl-Ile-Glu-Thr-Asp-AFC (IETD-AFC) and *N*-acetyl-Leu-Glu-His-Asp-AFC (LEHD-AFC). Soluble fractions (30 μg of protein) were incubated at 37 °C for 45 min in caspase buffer E (20 mM HEPES, pH 7.4, 50 mM NaCl, 0.2 mM EDTA, and 4 mM dithiothreitol) with 40 μM of the appropriate substrate. The nonspecific activity was measured in the presence of 10 μM of the appropriate caspase inhibitor *i.e.* the C-terminal aldehyde form (CHO) of the substrate (DEVD-CHO, IETD-CHO, and LEHD-CHO for caspases-3, -8 and –9, respectively). Fluorescence (excitation/emission: 400/505 nm for AFC and 380/460 nm for AMC) was measured in 96-well plates using a "Fusion" fluorometer (PerkinElmer Life Science). Enzyme activity was calculated using standard curves of AFC or AMC and expressed as the mean activity $\pm$ S.E. (picomole of AFC-AMC released$\cdot$min$^{-1}\cdot$mg^{-1} protein).

Degradation of Recombinant Caspases in Vitro and ex Vivo by Purified Calpain and Striatal Extracts from 3NP-treated Rats—We studied the *in vitro* proteolysis (1 h at 37 °C) of each recombinant human caspase (-3, -8, and -9) (50 ng for Western blot analysis and 10 ng for proteolysis activity assay, Biomol) by purified μ-calpain (0.2 units) in 100 μl of buffer D (with calcium). Cleavage of recombinant caspases was also studied after a 1-h incubation with cell-free extract of striatal homogenate from control or 3NP-treated rats (20 μg of protein). Digestion products were analyzed by 8–20% gradient SDS-PAGE followed by Western blot analysis. In addition, the functional effects of purified calpain and striatal extracts on recombinant caspases were quantitatively assessed by determining DEVDase and IETDase proteolytic activities related to active recombinant caspases-3 and -8, respectively. To detect the cleavage products of caspase-3 by calpain, we produced histidine-tagged and [^{35}S]methionine-labeled procaspase-3 using a rabbit reticulocyte lysate system (TNT quick coupled transcription/translation system, Promega) and a pET-15b-procaspase-3 construct. The pET-15b-procaspase-3 construct was generated as described previously (34). ^{35}S-Labeled caspase-3 protein was digested with recombinant caspase-8 (50 ng, Biomol) for maturation into its active form containing the p20 subunit. ^{35}S-Labeled p20 then was subjected to calpain digestion as described above. When stated, the calpain inhibitor CI-1 (10 μM) was added to the reaction. Reaction products were analyzed by SDS-PAGE. Following treatment with Amplify (Amersham Biosciences) and drying of gels, ^{35}S-labeled proteins were visualized by autoradiography.

Statistical Analysis—Results were expressed as the means $\pm$ S.E. Statistical analysis included Student's *t* test or ANOVA followed by a post hoc Scheffé *F*-test (StatView, version 5.0, Berkeley, CA).

RESULTS

Time Course of Behavioral, Histological, and Biochemical Changes Produced in the Striatum by Chronic 3NP Treatment—In agreement with previously reported experiments (22, 29, 30), the onset of overt motor symptoms (bilateral dystonia, uncoordinated movements, bradykinesia, and gait abnormalities) occurred on day 3 of 3NP treatment (Fig. 1*A*). In the experiment presented in Fig 1*A*, symptoms worsened on day 4 and reached their maximal severity on day 5. The analysis of SDH activity in the brain showed that after day 3 constant administration of 3NP produced a partial and constant mitochondrial defect very similar to that observed in HD (Fig. 1*B*). Histological evaluation of the striatum at various times during 3NP treatment showed overt tissue abnormalities in all of the animals after day 4. The nuclei of striatal cells were often fragmented as seen with Hoechst staining (Fig. 1*C*). Consistent with this finding, cytosolic fraction of striatal homogenates showed significant elevations in free oligonucleosome levels, indicating DNA fragmentation beginning at day 4 + 12 h and continuing thereafter (Fig. 1*D*).

We analyzed the "mitochondrial" apoptosis pathway in the striatum of 3NP-treated rats. The cellular distribution of cyt *c* in the striatum was modified during 3NP treatment as it is observed during apoptosis. Cyt *c* was barely detectable in the cytosolic fraction of striatal homogenates from control rats. In
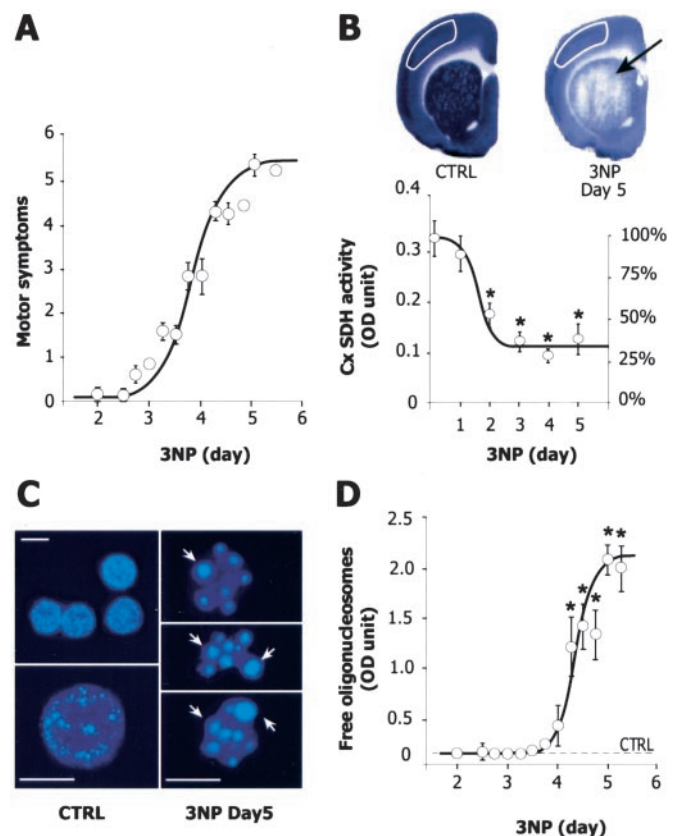
FIG. 1. **Mitochondrial defects and striatal degeneration produced by chronic 3NP administration.** Adult Lewis rats were systemically treated with 3NP and were assessed at the indicated time for motor symptoms and histological and biochemical changes. *A*, 3NP-induced motor symptoms. Obvious symptoms (hind limb dystonia) were observed on day 3 and worsened thereafter to reach a maximum on day 5. Each point corresponds to the mean value of motor index $\pm$ S.E. in 5–6 animals. For explanation of motor index, see "Materials and Methods." *B*, 3NP-induced inhibition of brain SDH activity. *Upper panels*, representative coronal rat brain sections revealed for SDH histochemistry from control (*CTRL*) and from rats at day 5 of 3NP treatment. Note the reduction of SDH activity in the entire brain. Pallor (*arrow*) within the striatum is due to ongoing neurodegeneration and 3NP-induced SDH blockade. *Lower panel*, the *curve* represents quantification of SDH activity in the cerebral cortex (see *white delineated regions* in *upper panel*), indicating that after 2–3 days of treatment, enzyme inhibition reaches ~65% and remains constant thereafter. Each point corresponds to the mean value $\pm$S.E. in 6–7 animals. *, $p < 0.0001$ compared with control, ANOVA, and post-hoc Scheffé *F*-test. *C*, nuclear abnormal morphology in the striatum of 3NP-treated rats. In control rats, Hoechst staining shows diffuse fluorescence through the nuclei of striatal neurons (*left panels*, CTRL). In 3NP-treated rats (day 5), the staining often shows fragmented nuclei (*right panels*, three representative examples) (scale bar, 10 μm). *D*, nuclear DNA fragmentation in the striatum during 3NP treatment evaluated by the presence of free oligonucleosomes in the soluble fraction of striatum homogenates. CTRLs are represented by the *dashed line*. Each point corresponds to the mean value $\pm$S.E. determined every 6 h in 5–6 animals. *, $p < 0.0001$ compared with control, ANOVA, and post-hoc Scheffé *F*-test.

contrast, cytosol fraction from 3NP-treated rats showed a marked and transient increase in cyt *c* on day 2, *i.e.* 3 days before the onset of striatal degeneration (Fig. 2*A*). Consistent with this observation, immunohistochemistry of cyt *c* with Nissl counterstaining showed accumulation of immunoreactivity in the perikarya of neurons (Fig. 2*B*). We next assessed the occurrence of caspase-9 and -3 activation in the 3NP model. Striatal cytosolic fractions from animals on days 2 and 3 showed a slight increase in the zymogen (p46) and processed form of caspase-9 (p34) compared with the base-line levels observed in controls (Fig. 2*C*). Measurement of caspase-9-related LEHDase activity in the striatum of 3NP rats showed
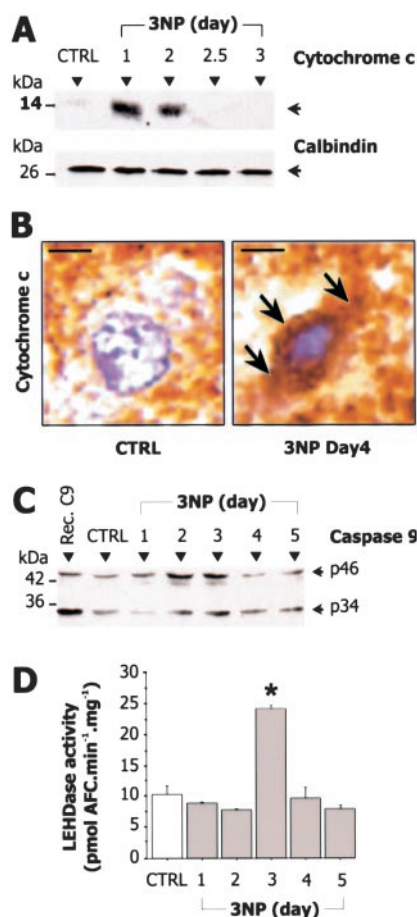
FIG. 2. **Activation of the mitochondrial pathway in the striatum of 3NP-treated rats.** Cyt *c* redistribution and transient caspase-9 activation during 3NP treatment. *A*, SDS-PAGE followed by Western blot for cyt *c* and calbindin D28K of striatal cytosol prepared from control (*CTRL*) and 3NP-treated rats. Note that in the cytosol of 3NP-treated rats, cyt *c* immunoreactivity transiently increases on days 1 and 2, whereas the neuronal marker calbindin remains stable, indicating an equal protein loading in each lane and consistent with an absence of neurodegeneration at these early time points. Results are typical of three independent experiments. *B,* immunohistochemistry of cytochrome *c* shows rare punctate labeling within the perikarya of striatal cells in control animals, whereas it increases in the perikarya in 3NP-treated rats (*arrows*). Nucleus is seen in *blue* after Cresyl violet counterstaining. *C,* Western blot of striatal homogenates for caspase-9 reveals a slight and transient increase in the zymogene (p46) and active form of caspase-9 (p34) on days 2 and 3. Recombinant activated caspase-9 (*Rec. C9*) mixed with control cytosol was loaded as a positive control in the *left lane*. *D*, LEHDase proteolytic activity during the 3NP treatment shows transient activation of caspase-9 at day 3. Each point corresponds to the mean value ±S.E. determined in triplicate and corresponds to 3–4 animals/day. *, $p < 0.0001$ compared with control, ANOVA, and post-hoc Scheffé *F*-test.

significant increase on day 3, consistent with a transient activation of caspase-9 (Fig. 2*D*). We next examined the status of caspase-3, which is activated downstream of caspase-9. Surprisingly, Western blot analysis showed an apparent loss of the active caspase-3 subunit p20 (seen as 17/19-kDa doublet) in the striatum of 3NP-treated animals on days 4 and 5 (Fig. 3*A*). In line with this finding, fluorometric measurements of DEVDase proteolytic activity in the striatal cytosolic fraction showed no activation of effector caspase-3 in 3NP-treated rats when compared with sham animals (Fig. 3*B*). Moreover, caspase-3-related proteolytic activity decreased during treatment (Fig. 3*B*).

As reported previously (22), Western blot analysis for fodrin (non-erythroid α-spectrin), a known substrate of both caspase-3 and calpain (35), showed a progressive accumulation of calpain-mediated fodrin breakdown products, which appeared as

a 150/145-kDa doublet, during 3NP treatment (Fig. 3*C*). The caspase-3-dependent 120-kDa breakdown product was not detected. On day 4, in the striatum of the 3NP-treated rats analyzed above for activation of caspases-3 and -9, the Ca^{2+}-dependent calpain-related activity revealed by the cleavage of the fluorogenic calpain substrate *N*-succinyl-LY-AMC was significantly increased ($+145\%$, $p < 0.0003$) compared with controls. In this experimental group of animals on day 5, calpain-related proteolytic activity was near control value ($+34\%$, non significant, Fig. 3*D*), whereas in other experiments calpain activity remained significantly increased on day 5.[2] Thus, there is a modest interexperiment variability with regards to the duration of calpain-related proteolytic activity due to 3-NP intoxication *in vivo*. Nevertheless, our results demonstrate the occurrence of activation of calpain associated with 3NP-induced mitochondrial defects.

Degradation of Caspase-9 and Caspase-3 by Calpain—Because during the course of 3NP-induced changes the loss of caspase-3 p20 subunit occurred despite cyt *c* redistribution and caspase-9 activation and was concurrent with the increase in calpain activity, we reasoned that calpain could be responsible for the lack of caspase-3 activation. To test this hypothesis in the striatum of 3NP-treated rats, we studied the effects of intracerebral infusion of the CI-1 on the endogenous levels of p20 and p34 subunits of caspases-3 and -9, respectively (Fig. 4). In this experiment, we analyzed the animals on day 5 of the 3NP treatment. In 3NP-treated rats, CI-1 infusion induced an increase in the levels of endogenous caspase-9 p34 subunit compared with control rats or 3NP-rats infused with CI-1 vehicle (Fig. 4*A*). *In vivo* CI-1 infusion also prevented the loss of endogenous caspase-3 p20 subunit induced by 3NP as shown by Western blot using an antibody recognizing the C-terminal domain of the p20 subunit of caspase-3 (Fig. 4*B*). Consistently, the endogenous DEVDase activity of striatal extracts was significantly reduced by 57% ($p < 0.006$) with the 3NP treatment. This reduction of activity was completely reversed to control values by *in vivo* CI-1 infusion (Fig. 4*C*). Altogether, our results demonstrated an inhibitory effect of calpain on caspase-3 activity. Therefore, we hypothesized that this inhibitory effect could result from a direct cleavage of caspases-9 and -3 by calpain.

Thus, we examined the degradation of the active subunits of caspases-9 and -3 in cell-free extracts prepared from the striatum of control and 3NP-treated rats on day 5 that were infused with CI-1 or vehicle. Striatal extracts from 3NP-treated rats infused with vehicle showed a significant increase in calpain activity compared with extract prepared from control rats (AMC released in $pmol\cdot min^{-1}\cdot mg^{-1}$ control: 20.51 ± 0.37; 3NP/vehicle: 29.37 ± 0.71, $+43\%$ *versus* control, $p < 0.0002$). In 3NP-treated rats injected with CI-1, calpain activity was significantly inhibited compared with controls (AMC released 5.92 ± 0.78 $pmol\cdot min^{-1}\cdot mg^{-1}$, $p < 0.0001$) and 3NP-treated rats injected with vehicle (data not shown). Recombinant caspases-9 and -3 were incubated with these extracts and then analyzed by Western blot. Extracts from 3NP rats induced a loss of recombinant caspase-9 subunit p34 (Fig. 5*A*), whereas control extracts produced no effect. Similarly, incubation of recombinant caspase-3 with striatal extract from 3NP-treated rats produced a loss of the caspase-3 subunit p20 (*i.e.* 19/17-kDa doublet) (Fig. 5*B*). In line with this finding, DEVDase activity of the recombinant caspase-3 was reduced to 68% following incubation with striatal extracts from 3NP-treated rats as compared with striatal extracts from control rats (Fig. 5*B*).

---

[2] D. Blum, M. F. Beal, L. Yang, N. Bizat, J.-M. Hermel, and E. Brouillet, unpublished results.

FIG. 3. **3NP treatment induces a decrease of active caspase-3 and an increase in calpain activity *in vivo*.** Striatal cytosol fractions were prepared from control (*CTRL*) and 3NP-treated rats (*i.e.* days 1–5). *A*, SDS-PAGE followed by Western blot (chemiluminescence detection with amplification) for active caspase-3 of striatal cytosol fractions. *B*, decreased caspase 3-like DEVDase proteolytic activity during 3NP treatment. *C*, SDS-PAGE followed by Western blot for fodrin of membrane fractions prepared from striatum of control (*CTRL*) and 3NP-treated rats. Note the typical calpain-mediated breakdown products of fodrin appearing as a doublet (150/145 kDa). *D*, Ca^{2+}-dependent calpain-related proteolytic activity (cleavage of *N*-succinyl-LY-AMC) increases significantly in the striatum of 3NP-treated animals. Note that the increase in calpain activity is followed by progressive decline in immunoreactivity for the caspase-3 p20 subunit and DEVDase-related activity. Data are means ± S.E. *, $p < 0.02$; **, $p < 0.0003$ compared with control, ANOVA, and post-hoc Scheffé *F*-test.
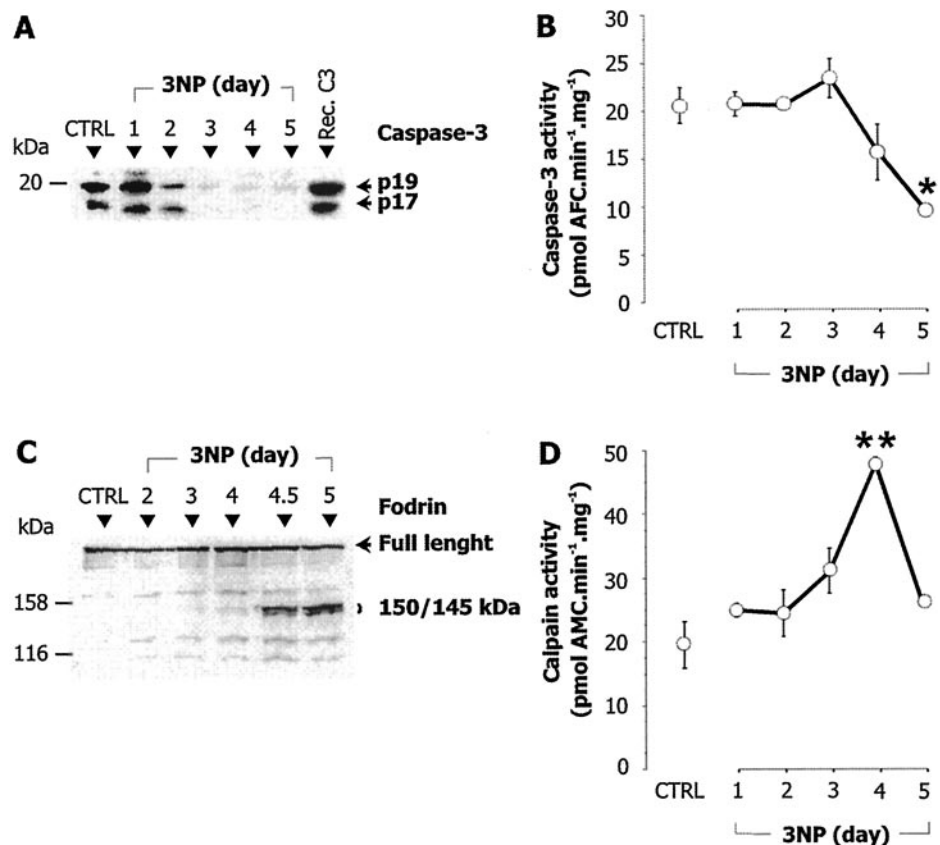
This loss of detection of active/processed caspases-3 and -9 produced by striatal extract of 3NP-treated rats was significantly reduced by the addition of the selective calpain inhibitor z-LL-CHO *in vitro* or by delivering *in vivo* CI-1 during the 3NP treatment (Fig. 5). Similarly, the loss of DEVDase activity induced by striatal extracts was also prevented by z-LL-CHO incubation and CI-1 treatment (Fig. 5). These results indicated that calpain could be responsible for the degradation of caspases-9 and -3 in the striatum of 3NP-treated rats, probably through a cleavage of the active/processed forms of the caspases.

We next assessed the possibility of a direct *in vitro* cleavage of recombinant caspases-9 and -3 by incubation with purified μ-calpain. After SDS-PAGE resolution of the products, Western blot analyses showed that calpain degraded the p34 subunit of human active recombinant caspase-9 (Fig. 6*A*), in agreement with previous reports (25). After incubation with μ-calpain, active recombinant caspases-3, *i.e.* the p17/19 doublet, was no longer detected by Western blot using an antibody recognizing the C-terminal domain of the p20 subunit (Fig. 6*B*). No caspase-3 fragment smaller than 17 kDa was detected, suggesting a digestion of this epitope. The cleavage of active recombinant caspase-3 by μ-calpain was correlated with a loss of its DEVDase proteolytic activity (Fig. 6*C*). Both the loss of immunoreactivity by Western blot and DEVDase activity were reversed by incubation of calpain with its inhibitor Cl-1. In contrast, using the same incubation conditions, calpain produced no effects upon the IETDase activity of recombinant active caspase-8 (data not shown). Because we showed that antibodies directed against the C-terminal domain of p20 could no longer recognize the protein after calpain-mediated cleavage and that cleavage produced a loss of proteolytic activity, we hypothesized that the site of cleavage on p20 was near its catalytic site at the C terminus of the peptide and that the C-terminal domain of p20 interacts with calpain. To test this

hypothesis, we studied whether a synthetic peptide corresponding to the C-terminal 12 amino acids of p20 (Ct12p20) could inhibit μ-calpain activity detected by cleavage of *N*-succinyl-LY-AMC at 150 μM. We found that the Ct12p20 peptide inhibited calpain activity with an apparent IC_{50} of 106 μM and with 100% inhibition at 1 mM (Fig. 6*D*). The scramble peptide produced no inhibition at 1 mM. Interestingly, a Ct12p20 peptide in which leucine 168 was substituted by lysine (Ct12p20-L168K) produced no inhibition at 1 mM. These results further suggested that the interaction between Ct12p20 and calpain was of low affinity but specific.

We next studied the calpain-dependent cleavage of recombinant histidine tagged procaspase-3 and caspase-3 p20 subunit, which were radiolabeled using *in vitro* translation assay in presence of [^{35}S]methionine (Fig. 7). The procaspase-3 migrated at an apparent molecular mass of 36 kDa corresponding to the theoretical molecular mass of 32 kDa of procaspase-3 plus the histidine tag. The 36-kDa procaspase-3 was cleaved by μ-calpain *in vitro*, leading to a main breakdown product of 30 kDa, consistent with the cleavage site in the N-terminal part of procaspase-3 reported previously (24, 27). We then tested whether calpain also cleaved the p20 active subunit. To do so, we first obtained a radiolabeled caspase-3 p20 subunit after maturation of the procaspase-3 by caspase-8 (Fig. 7). The p20 subunit migrated near 19 kDa. A larger peptide of ~25 kDa was also produced, possibly corresponding to procaspase-3 cleaved only in its N-terminal domain (Asp-28). Subsequent incubation of the p20 subunit of caspase-3 with calpain produced the disappearance of the 19-kDa band leading to a smaller fragment of 18 kDa. Note that we could not resolve proteins of molecular mass lower than 12 kDa that may be generated in our experimental conditions.
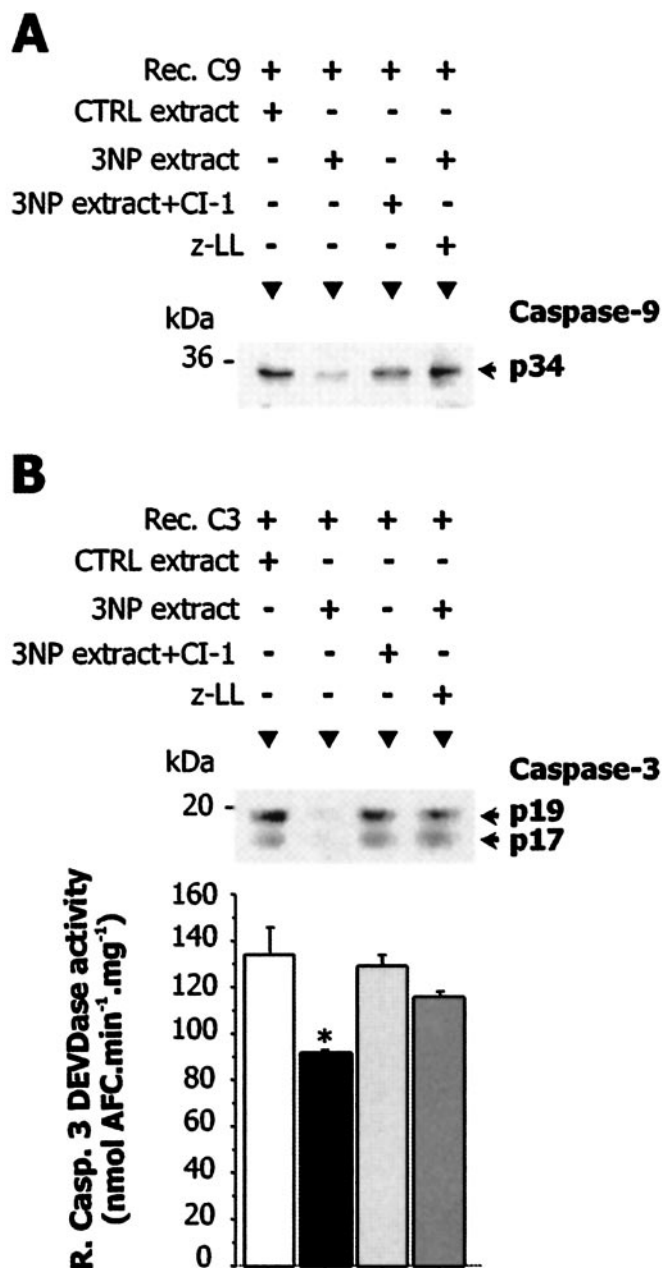
Altogether, we demonstrated that the p20 active form of caspase-3 is cleaved by calpain near its catalytic site, inactivating caspase-3 proteolytic activity.
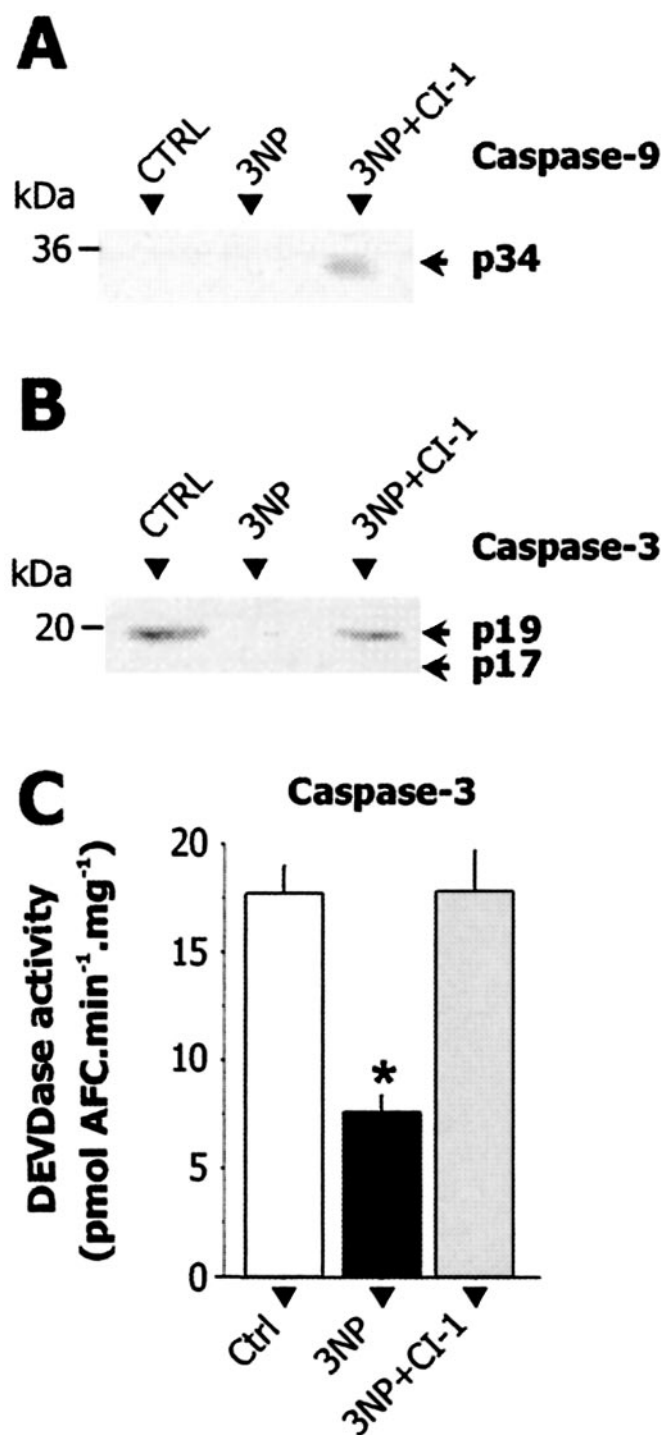
FIG. 4. **Blockade of calpain by Cl-1 modifies the 3NP-induced loss of endogenous processed caspase-3 and caspase-9 *in vivo*.** Striatal extracts from control rats (*CTRL*) and from rats treated with 3NP for 5 days (*3NP*) or with 3NP plus calpain inhibitor I (*3NP+Cl-1*) were analyzed by Western blot for caspase-9 (*A*) and caspase-3 (*B*) and for caspase-3 DEVDase activity (*C*). Intracerebral delivery of CI-I in 3NP rats induced an accumulation of the endogenous active caspase-9 and prevented the loss of active caspase-3 immunoreactivity and caspase-3 activity in the striatum. Data are means ± S.E. *, $p < 0.006$ compared with control, ANOVA, and post-hoc Scheffé *F*-test.

FIG. 5. **Effects of cell-free extracts from 3NP-treated rats on recombinant caspases-3 and -9.** Cell-free extracts prepared from striatum of control (*CTRL extract*) or 3NP-treated rats (*3NP extract*) treated or not with calpain inhibitor I (*Cl-1*) *in vivo* were incubated with recombinant caspase-3 or -9 (*Rec. C9* and *Rec. C3*, respectively). Cell-free extracts from 3NP-treated rats were incubated with or without calpain inhibitor z-LL-CHO (*z-LL*). Following SDS-PAGE, we performed Western blots for caspase-9 (*A*) and caspase-3 (*B, upper panel*). For caspase 3 blots, we used an antibody selectively recognizing the 12 C-terminal amino acids of the p20 subunit. The DEVDase proteolytic activity of active recombinant caspase-3 was also evaluated in the same samples as described above (*B, lower panel*). Note that recombinant caspases-3 and -9 remain stable in the presence of CTRL extract. Recombinant caspases-3 and -9 are degraded by extracts of 3NP-treated rats. This degradation is prevented *in vitro* by z-LL or with striatal extracts prepared from rats treated with Cl-1 *in vivo*. Data are the means ± S.E. *, $p < 0.003$ compared with control and CI-1, ANOVA, and post-hoc Scheffé *F*-test.

DISCUSSION

In this study, we used our chronic 3NP intoxication model of neurodegeneration in rat to further study cellular changes and biochemical pathways leading to striatal cell death during mitochondrial defects (22). We showed that cytochrome *c* redistribution and transient caspase-9 processing occur at the be-

ginning of the 3NP treatment. The fact that these events occurred 2–3 days before cell degeneration (*i.e.* nuclei fragmentation) suggest that *in vivo* primary blockade of complex II activity by 3NP leads to early activation of the so-called caspase-dependent mitochondrial pathway as seen in *bona fide* apopto-
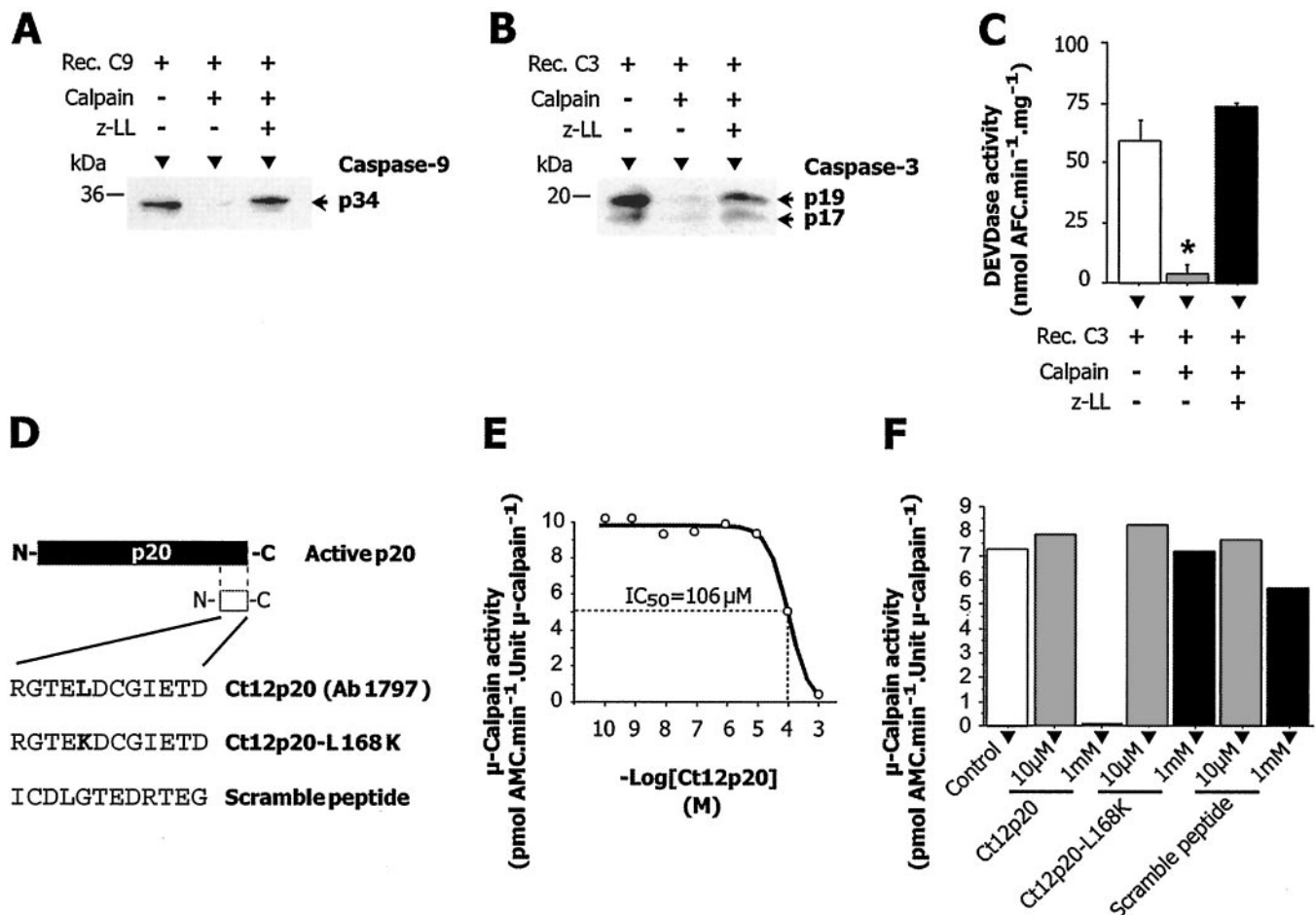
FIG. 6. **μ-Calpain-degrades active forms of caspase-3 and caspase-9 *in vitro*.** After *in vitro* incubation of recombinant caspase-3 (*Rec. C3*) and -9 (*Rec. C9*) with purified μ-calpain with or without calpain inhibitor z-LL-CHO (*z-LL*), we analyzed the digestion products by SDS-PAGE followed by Western blot for activated caspase-9 revealing the p34 subunit (*A*) and for activated caspase-3 revealing the p20 subunit appearing as p17-p19 doublet (*B*). No smaller caspase-9 fragment was detected below 34 kDa. No smaller caspase-3 fragment was detected below 17 kDa. The antibody directed against active caspase-3 recognizes the 12 C-terminal amino acids of p20. Note that caspase-9 p34 and caspase-3 p20 are degraded by incubation with μ-calpain. This degradation is prevented by the incubation of μ-calpain with its inhibitor z-LL. *C*, the DEVDase activity of Rec. C3 is almost suppressed by calpain. This calpain effect is prevented by z-LL. Assays were performed in triplicate. *D*, representation of the p20 subunit of active caspase-3 (*p20*) and sequence of the 12 C-terminal amino acids of its Ct12p20 domain against which the antibody Ab1797 was raised. Sequence of the modified Ct12p20 peptide with the leucine 168 substituted for a lysine (Ct12p20-L168K). *E*, concentration-response inhibition of calpain activity by the Ct12p20 peptide. The IC$_{50}$ of this inhibition (106 μM) suggests the specific interaction of the C-terminal domain of caspase-3 with calpain. *F*, activity of purified μ-calpain in presence of Ct12p20, Ct12p20-L168K, and the scrambled peptide. Only Ct12p20 at 1 mM inhibits μ-calpain activity. Results are expressed as mean $\pm$ S.E. *, $p < 0.005$ compared with control, ANOVA, and post-hoc Scheffé F-test.

sis. In apoptosis or accidental cell death, caspase-9 activation is often followed by downstream activation of the effector caspase-3 (36). Unexpectedly, this study shows that this is not the case in our 3NP model of striatal neurodegeneration.

In the brain of control rats, we detected base-line or "physiological" levels of the activated caspase-3 p20-subunit as well as DEVDase activity that were similar to baseline levels of active caspase-3 shown by others (37). Little is known regarding the "physiological" levels of caspase activity in the normal adult rat brain. One possibility is that apparent basal levels of active caspase-3 in the normal brain is due, at least in part, to post-mortem processing of the brain tissue. However, we found caspase-3-related DEVDase activity in rat striatal samples prepared using freeze-clamp methods and we detected the caspase-3 p20 subunit by Western blot in the striatum of non-human primates fixed using transcardial paraformaldehyde perfusion.[3] These procedures minimize post-mortem modification of proteins. In line with this finding, there is some evidence of caspase activity in normal brain related to synaptic plas-

ticity (38) and to physiological processing of proteins such as huntingtin (39).

The 3NP treatment produced neither an increase of caspase-3 p20 concentration nor caspase-3-related activity. On the contrary, levels of detectable p20 subunit and DEVDase activity decreased during the 3NP treatment. We found that the apparent loss of the active caspase-3 p20 subunit followed a prominent increase in calpain activity, another important cell death effector protease (35). Thus, we examined whether the regulation of caspases-9 and -3 could involve calpain.

In this respect, we found that purified calpain could degrade processed caspase-9 subunit p34 *in vitro*. Additionally, using cell-free extracts, we showed that endogenous active calpain from the striatum of 3NP-treated rats could degrade the processed recombinant caspase 9 p34 subunit. This is consistent with results reported by others (25, 26), which showed that *in vitro* purified calpain cleaved procaspase-9 at four main cleavage sites including one in the p34 subunit prodomain. These authors showed that calpain cleaves procaspase-9, hampering subsequent processing into its active form. In the 3NP model, caspase-9 activation is transiently detected on day 3, levels of p34 subunit of processed caspase-9 returning to base-line levels

---

[3] M. F. Beal, L. Yang, F. Condé, N. Bizat, J.-M. Hermel, P. Hantraye, and E. Brouillet, unpublished results.
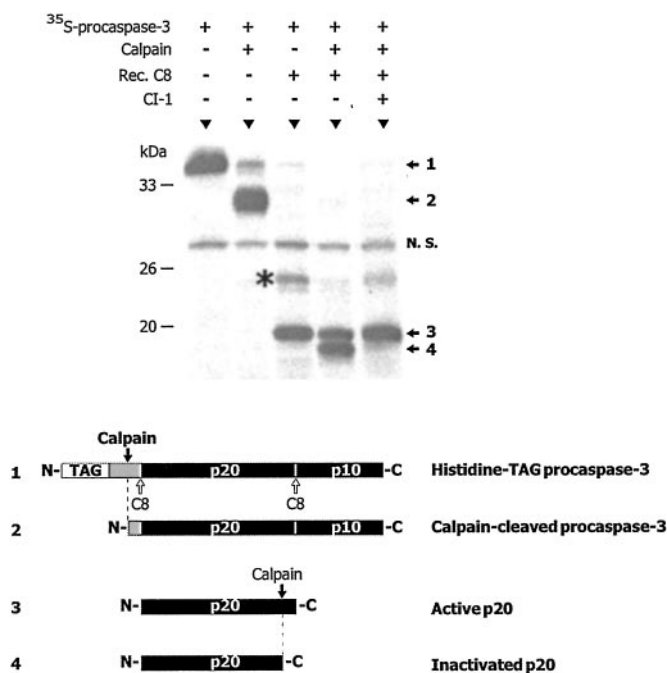
FIG. 7. **Caspase-3 is cleaved by calpain *in vitro*.** Histidine-tagged procaspase-3 (36 kDa) was labeled with [^{35}S]methionine and incubated with calpain and/or caspase-8 in the presence of Cl-1 or not. *Upper panel*, the cleaved products were resolved by a SDS-PAGE and then dried and exposed for autoradiography. Procaspase-3 (*1*) is cleaved (*open arrows*) by caspase-8 (*C8*) to produce an active caspase-3 p20 fragment (*3*). This caspase-3 p20 subunit is further cleaved by calpain (*black arrows*) into a breakdown product of 18 kDa (*4*). Calpain also cleaved the procaspase-3 to produce a 30-kDa peptide (*2*). The caspase-8 cleavage of procaspase-3 (*open arrows*) generates a larger peptide of ~25 kDa (*asterisk*) that seems to be unstable and that is further cleaved to generate the p20 active form. This 25-kDa peptide may possibly correspond to procaspase-3 cleaved only in its N-terminal domain (Asp-28). The nonspecific (*N.S.*) band resolved at ~28 kDa appears to be a contaminant peptide unrelated to caspase-3. The cleavage of caspase-3 p20 by calpain is inhibited by adding Cl-1 (10 μM). *Numbers* in the *lower panel* correspond to the aligned schemes of peptides present in the experiment described above. *Dashed lines* represent putative calpain cleavage site.

on day 5. Interestingly, we showed that blocking calpain activity *in vivo* during 3NP treatment led to an increase in the levels of p34 on day 5 as compared with control levels. This finding strongly suggests that during 3NP-induced degeneration, calpain hampers caspase-9 activation (Fig. 8). To our knowledge, this is the first evidence that calpain could down-regulate the activation of caspase-9 in the living brain during a neurodegenerative process.

The calpain-mediated inactivation of caspase-9 may be at least partly responsible for the down-regulation of active caspase-3 in the 3NP model. However, we identified another potential mechanism that could also contribute to hamper caspase-3 activation. We showed that the active form of caspase-3 was cleaved by calpain, leading to a loss of its DEVDase activity. Western blot analysis of p20 breakdown products using different antibodies showed that the p20 subunit was cleaved in its C-terminal region. Cleavage of p20 by calpain was confirmed by experiments using radiolabeled recombinant p20. These data together with the analysis of the radiolabeled recombinant p20-cleaved products by calpain and the inhibition of calpain activity by the 12 C-terminal amino-acids of p20 led us to propose that the calpain cleavage site on p20 is located at ~10 amino acids from Asp-175 of the C terminus. This is consistent with the resulting loss of activity, because the cysteine of the catalytic site is very close (Cys-163). Although calpain lacks a strict consensus cleavage site, calpain often
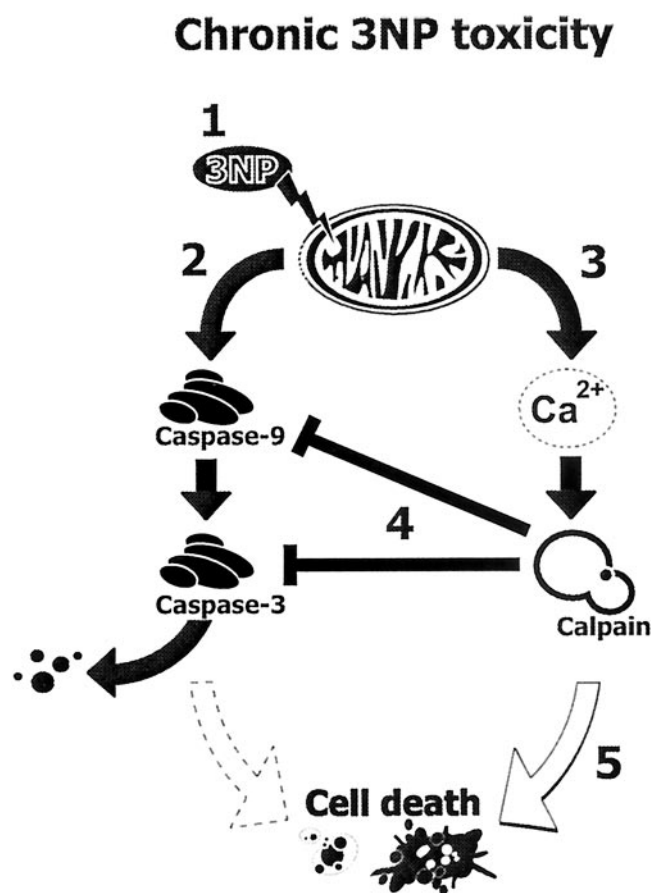

FIG. 8. **Scheme pathways of the chronic 3NP toxicity.** 3NP (*1*) specifically blocks the mitochondrial succinate dehydrogenase leading to the activation of two parallel pathways, the mitochondrial pathway involving caspase-9 (*2*) and the calpain pathway triggered by cytoplasmic [Ca^{2+}] increase (*3*). Activated caspase-9 would process the effector caspase-3, which should lead to apoptotic cell death. In parallel, the increase in intracellular [Ca^{2+}] concentration could activate μ-calpain and possibly m-calpain at the same time. The calpains then may block the caspase-9/-3 apoptotic pathways at least in part through cleavage of the active caspases (*4*) and lead to cell death through still unraveled mechanisms (*5*).

cleaves its substrates in position P2 of a leucine, isoleucine, or valine (35). Therefore, it could be assumed that calpain cleaves p20 at position Leu-168 and this is supported by our observation that the L168K substitution blocks the ability of the C-terminal domain of p20 to inhibit μ-calpain. Unfortunately, the precise calpain cleavage site on p20 is not established and we did not succeed in isolating the small breakdown product of p20 after calpain digestion for N-terminal sequencing. The existence of one calpain-dependent cleavage site in the N-terminal prodomain of caspase-3 (residue Ser-7) was described previously by Wolf and collaborators (27). It should be noted that the calpain cleavage site in caspase-3 p20 is not sensitive to calpain in the procaspase-3. On the other hand, three-dimensional reconstruction of active caspase-3 structure indicates that the C-terminal region of p20 is highly exposed to the external environment (40), which is compatible with the possibility that calpain may easily interact with this domain. In consideration of all of the above, our study demonstrates that calpain cleaves the active p20 subunit of caspase-3 at a site near its C-terminal region but not the p20 domain of the procaspase-3.

Our data further documents the potential mechanisms underlying a cross-talk between calpain and caspases-9 and -3 pathway. During the cell death process involving calpain, activation of caspases-3 and 9 could be regulated by inactivation

of their proform, blocking further maturation (25–27). Our results suggest that, in addition, calpain can directly cleave the active/processed form of caspase-3, thus adding a new fork to the complicated pathways leading to cell death (Fig. 8). This calpain-mediated cleavage of p20 could at least partly explain how calpain could predominate during striatal cell death induced by 3NP (22) or other toxins such as NMDA (26).

It is possible that the novel mechanism through which calpain regulates directly caspase-3 proteolytic activity could be involved in neurodegenerative disorders associated with partial mitochondrial defects. Given that 3NP toxicity replicates many biochemical, histological, and behavioral features of HD in laboratory animals (21), it is tempting to speculate that the caspase-9/-3 pathway may be down-regulated by calpain in the striatum of HD patients. This hypothesis awaits confirmation by observations on human samples.

REFERENCES

1. Beal, M. F. (2000) *Trends Neurosci.* **7,** 298–304
2. The Huntington's Disease Collaborative Research Group. (1993) *Cell* **72,** 971–983
3. Harper, P. S. (1991) *Huntington's Disease*, W. B. Saunders Co., Philadelphia, PA
4. DiFiglia, M. (1990) *Trends Neurosci.* **13,** 286–289
5. Beal, M. F., Kowall, N. W., Ellison, D. W., Mazurek, M. F., Swartz, K. J., and Martin, J. B. (1986) *Nature* **321,** 168–171
6. Ferrante, R. J., Kowall, N. W., Cipolloni, P. B., Storey, E., and Beal, M. F. (1993) *Exp. Neurol.* **119,** 46–71
7. Laforet, G. A., Sapp, E., Chase, K., McIntyre, C., Boyce, F. M., Campbell, M., Cadigan, B. A., Warzecki, L., Tagle, D. A., Reddy, P. H., Cepeda, C., Calvert, C. R., Jokel, E. S., Klapstein, G. J., Ariano, M. A., Levine, M. S., DiFiglia, M., and Aronin, N. (2001) *J. Neurosci.* **21,** 9112–9123
8. Zeron, M. M., Hansson, O., Chen, N., Wellington, C. L., Leavitt, B. R., Brundin, P., Hayden, M. R., and Raymond, L. A. (2002) *Neuron* **33,** 849–860
9. Albin, R. L., and Greenamyre, J. T. (1992) *Neurology* **42,** 733–738
10. Beal, M. F. (1992) *Ann. Neurol.* **31,** 119–130
11. Gu, M., Gash, M. T., Mann, V. M., Javoy-Agid, F., Cooper, J. M., and Shapira, A. H. (1996) *Ann. Neurol.* **39,** 385–389
12. Browne, S. E., Bowling, A. C., Mac Garvey, U., Baik, M. J., Berger, S. C., Muqit, M. K., Bird, E. D., and Beal, M. F. (1997) *Ann. Neurol.* **41,** 646–653
13. Jenkins, B. G., Rosas, H. D., Chen, Y. C. I., Makabe, T., Myers, R., MacDonald, M., Rosen, B. R., Beal, M. F., and Koroshetz, W. J. (1998) *Neurology* **50,** 1357–1365
14. Sawa, A., Wiegand, G. W., Cooper, J., Margolis, R., Sharp, A. H., Lawler, J. F., Greenamyre, J. T., Snyder, S. H., and Ross, C. (1999) *Nat. Med.* **5,** 1194–1198
15. Panov, A. V., Gutekunst, C. A., Leavitt, B. R., Hayden, M. R., Burke, J. R., Strittmatter, W. J., and Greenamyre, J. T. (2002) *Nat. Neurosci.* **5,** 731–736
16. Coles, C. J., Edmonson, D. E., and Singer, T. P. (1979) *J. Biol. Chem.* **255,** 772–4780
17. Brouillet, E., Guyot, M. C., Mittoux, V., Altairac, S., Condé, F., Palfi, S., and Hantraye, P. (1998) *J. Neurochem.* **70,** 794–805
18. Beal, M. F., Brouillet, E., Jenkins, B., Ferrante, R. J., Kowall, N., Miller, J., Storey, E., Srivastava, R., Rosen, B. R., and Hyman, B. T. (1993) *J. Neurosci.* **13,** 4181–4192
19. Brouillet, E., Hantraye, P., Ferrante, R. J., Dolan, R., Leroy-Willig, A., Kowall, N. W., and Beal, M. F. (1995) *Proc. Natl. Acad. Sci. U. S. A.* **92,** 7101–7109
20. Palfi, S., Ferrante, R. J., Brouillet, E., Beal, M. F., Dolan, R., Guyot, M. C., Peschanski, M., and Hantraye, P. (1996) *J. Neurosci.* **16,** 3019–3025
21. Brouillet, E., Condé, F., Beal, M. F., and Hantraye, P. (1999) *Prog. Neurobiol.* **59,** 427–458
22. Bizat, N., Hermel, J. M., Boyer, F., Créminon, C., Ouary, S., Escartin, C., Hantraye, P., Krajewski, S., and Brouillet, E. (2003) *J. Neurosci.* **23,** 5020–5030
23. Gafni, J., and Ellerby, L. M. (2002) *J. Neurosci.* **22,** 4842–4849
24. Blomgren, K., Zhu, C., Wang, X., Karlsson, J. O., Leverin, A. L., Bahr, B. A., Mallard, C., and Hagberg, H. (2001) *J. Biol. Chem.* **276,** 10191–10198
25. Chua, B. T., Guo, K., and Li, P. (2000) *J. Biol. Chem.* **275,** 5131–5135
26. Lankiewicz, S., Marc Luetjens, C., Truc Bui, N., Krohn, A. J., Poppe, M., Cole, G. M., Saido, T. C., and Prehn, J. H. (2000) *J. Biol. Chem.* **275,** 17064–17071
27. Wolf, B. B., Goldstein, J. C., Stennicke, H. R., Beere, H., Amarante-Mendes, G. P., Salvesen, G. S., and Green, D. R. (1999) *Blood* **94,** 1683–1692
28. Brouillet, E., Jenkins, B., Hyman, B., Ferrante, R. J., Kowall, N. W., Srivastava, R., Roy, D. S., Rosen, B., and Beal, M. F. (1993) *J. Neurochem.* **60,** 356–359
29. Garcia, M., Vanhoutte, P., Pages, C., Besson, M. J., Brouillet, E., and Caboche, J. (2002) *J. Neurosci.* **22,** 2174–2184
30. Mittoux, V., Ouary, S., Monville, C., Lisovoski, F., Poyot, T., Conde, F., Escartin, C., Robichon, R., Brouillet, E., Peschanski, M., and Hantraye, P. (2002) *J. Neurosci.* **22,** 4478–4486
31. Qin, Z. H., Wang, Y., Kikly, K. K., Sapp, E., Kegel, K. B., Aronin, N., and DiFiglia, M. (2001) *J. Biol. Chem.* **276,** 8079–8086
32. Krajewski, S., Krajewska, M., Ellerby, L. M., Welsh, K., Xie, Z., Deveraux, Q. L., Salvesen, G. S., Bredesen, D. E., Rosenthal, R. E., Fiskum, G., and Reed, J. C. (1999) *Proc. Natl. Acad. Sci. U. S. A.* **96,** 5752–5757
33. McDonald, M. C., Mota-Filipe, H., Paul, A., Cuzzocrea, S., Adbelrahman, M., Harwood, S., Plevin, R., Chatterje, P. K., Yaqoob, M. M., and Thiemermann, C. (2001) *FASEB J.* **15,** 171–186
34. Cryns, V. L., Bergeron, L., Zhu, H., Li, H., and Yuan, J. (1996) *J. Biol. Chem.* **49,** 31277–31282
35. Wang, K. (2000) *Trends Neurosci.* **23,** 20–26
36. Thornberry, N. A., and Lazebnik, Y. (1998) *Science* **281,** 1312–1316
37. Benchoua, A., Guegan, C., Couriaud, C., Hosseini, H., Sampaio, N., Morin, D., and Onteniente, B. (2001) *J. Neurosci.* **21,** 7127–7134
38. Dash, P. K., Blum, S., and Moore, A. N. (2000) *Neuroreport* **11,** 2811–2816
39. Kim, Y. J., Yi, Y., Sapp, E., Wang, Y., Cuiffo, B., Kegel, K. B., Qin, Z. H., Aronin, N., and DiFiglia, M. (2001) *Proc. Natl. Acad. Sci. U. S. A.* **98,** 12784–12789
40. Rotonda, J., Nicholson, D. W., Fazil, K. M., Gallant, M., Gareau, Y., Labelle, M., Peterson, E. P., Rasper, D. M., Ruel, R., Vaillancourt, J. P., Thornberry, N. A., and Becker, J. W. (1996) *Nat. Struct. Biol.* **3,** 619–625

Nicolas Bizat, Jean-Michel Hermel, Sandrine Humbert, Carine Jacquard, Christophe Créminon, Carole Escartin, Frédéric Saudou, Stan Krajewski, Philippe Hantraye and Emmanuel Brouillet

Access the most updated version of this article at doi: 10.1074/jbc.M305057200

Alerts:
- When this article is cited
- When a correction for this article is posted

Click here to choose from all of JBC's e-mail alerts

This article cites 39 references, 18 of which can be accessed free at
http://www.jbc.org/content/278/44/43245.full.html#ref-list-1